Accuracy and realism of CMIP6 candidate models in capturing dry, moist, and extreme precipitation anomalies in the Laurentian Great Lakes.

Tasmeem Jahan Meem[1], Elizabeth K. Carter[1,2]*, Tripti Bhattacharya[2], Stephen B Shaw[3]

[1]Department of Civil and Environmental Engineering, Syracuse University, NY 13244, United States

[2]Department of Earth and Environmental Science, Syracuse University, NY 13244, United States

[3]Department of Environmental Resources Engineering, SUNY College of Environmental Science and Forestry, NY 13244, United States

*Corresponding author, ekcarter@syr.edu

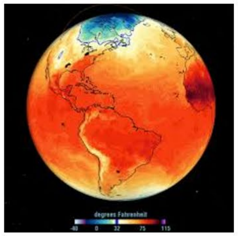

Climate Change will modify regional hydroclimate in two ways:

Thermodynamically

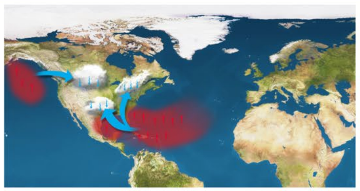

"Wet gets wetter, dry gets drier"
Saturation vapor pressure increases with temperature

Dynamically

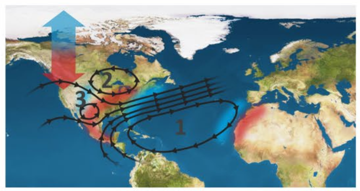

Wet and dry locations can shift
Atmospheric circulation patterns change

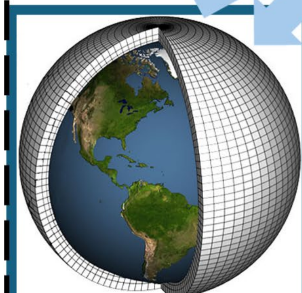

For reliable forecasts, CESMs must accurately parameterize regional precipitation dynamics and hydroclimatic circulation.

Accuracy and realism of CMIP6 models: future precipitation in the Great Lakes

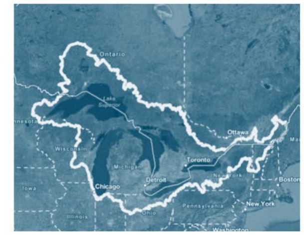

Thermodynamic accuracy

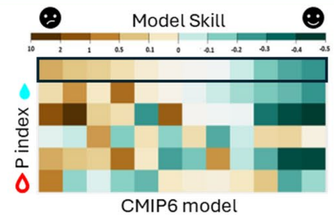

Fidelity at extreme P metrics:
- Dry indices
- Wet indices
- Extreme indices

Dynamical realism

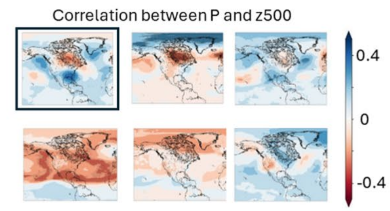

Captures regional hydroclimatic circulation anomalies:
- PNA
- NASH

The two most accurate and realistic models predict longer dry stretches; shorter wet stretches in Great Lakes in the summer.

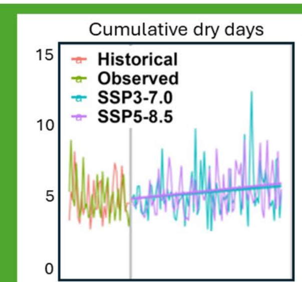

Abstract

The Great Lakes are the world's largest freshwater system, and understanding how Great Lakes precipitation dynamics will be modified by climate change is of critical importance. As the Great Lakes straddles a semi-arid to humid transitional region, trustworthy precipitation predictions must be generated by models that can accurately capture both thermodynamical and dynamical drivers of regional hydroclimatological variability in historical runs. In this study, precipitation simulations from 12 CMIP6 models, representing the full range of variability in numeric representation of North American climate, are evaluated for accuracy in capturing historic seasonal wet, dry, and extreme precipitation anomalies in the Great Lakes region. Based on historical accuracy, a subset of candidate models is selected. Simple statistical methods are used to explore the relationships between cumulative seasonal precipitation anomalies and mid-level circulation anomalies, both in observations and in historical model runs. Historic observations suggest that the Pacific North American pattern and North Atlantic subtropical high are important components of summertime hydroclimatic circulation in the region. The two models which most accurately characterize a range of precipitation anomalies replicate these hydroclimatic circulation patterns with the highest fidelity. These two most accurate and physically plausible models are in consensus in predicting an increasing length of dry spells, and decreasing duration of wet days, suggesting increased drought risk under climate change. They diverge between negative and neutral trends in maximum daily precipitation and total precipitation. Implications for water resources management and statistical downscaling studies are discussed.

Keywords: CMIP6; Great Lakes; extreme precipitation; climate dynamics; climate change; CESM realism

1. Introduction

The Laurentian Great Lakes contain 21% of the world's surface freshwater, making them the largest surface freshwater system on earth. The Great Lakes supply drinking water to 8% of the United States and 30% of the Canadian population. Nearly 25% of Canadian agricultural production and 7% of American agricultural production occurs in the Great Lakes watershed. The Great Lakes surface water system, including the Saint Lawrence River, are essential inland navigation routes for the shipping industry. Since 1959, over $375 billion in commodities have traveled through the Great Lakes seaway on transport to or from the United States and Canada (United States EPA 2025). The management of the Great Lakes system involves international coordination between the United States and Canada by way of the International Joint Commission, as well as state and local governments across eight US states and two Canadian provinces. With so many stakeholders involved, and so much at stake, accurate information about current and future hydrologic conditions in the Great Lakes basin is essential to the coordination of successful human enterprise across North America.

Seager et al. (2010) demonstrate that global warming will modify local hydrologic variability both thermodynamically and dynamically, and that the fidelity of characterization of both mechanisms must be considered when evaluating the realism of local hydrologic predictions under climate change (Seager et al. 2014). Thermodynamically, warmer air temperatures expected under global warming drive higher saturation vapor pressures. According to the Clausius-Clapeyron relationship, as average air temperatures increase under climate change, the maximum mass of water that can be in the atmosphere will increase as well, by about 7% for every 1° C temperature increase (Trenberth 2011; Allan et al. 2020). Temperature-modulated increases in saturation vapor pressure will are theoretically associated with both an increase in precipitation rates (increased in the total mass and intensity of precipitation delivered during convection) and evaporation rates (an increase in the humidity gradient between moist land surfaces and warm dry air will increase rates of terrestrial drying). Often called "wet gets wetter, dry gets drier," thermodynamic intensification of the hydrologic cycle under global warming is expected to increase the net moisture supply in humid climates and increase the net aridity in arid climates (Trenberth 2011; Shaw et al. 2011).

Dynamically, the spatial distribution of humid and arid climates is determined by stable patterns in global atmospheric circulation. Atmospheric currents route moisture-enriched air from ocean basins over terrestrial landmasses, determining the spatial distribution of arid and humid landscapes at the continental scale (Gimeno et al. 2010). Atmospheric circulation patterns are complex, scale-dependent functions of earth's axial rotation, earth's orbit around the sun, thermal gradients in the oceans (which are modified by oceanic circulation), thermal gradients between land-sea interfaces, diabatic heating/cooling associated with internal atmospheric processes, and local landscape forcings such as land cover, elevation, and the presence of freshwater bodies. Dynamical shifts in hydroclimatology, that occur when increasing air temperatures modify large-scale atmospheric circulation patterns by way of modified thermal and osmotic gradients within oceans and across land masses, are projected to shift the geographic and seasonal distribution of terrestrial moisture supply. Taken in tandem, thermodynamic and dynamic shifts in hydroclimatology are expected to shift both the intensity of precipitation and evapotranspiration, and the space-time distribution of humidity and aridity, across continental landmasses (Seager et al. 2010, 2014; O'Gorman 2015; Allan et al. 2020).

There is broad consensus on the impact of thermodynamic intensification of the hydrologic cycle across different earth system models. An increase in temperature increases the moisture holding capacity of the atmosphere. This moisture availability will result in an increase in the intensity of precipitation, though the average global precipitation will be constrained by the energy availability for evaporation and convection (Trenberth 1999; Allen and Ingram 2002). Across all latitude bands, the extreme precipitation sensitivity to temperature is found to be positive, albeit with different magnitudes locally (O'Gorman 2015; Pfahl et al. 2017). The increase in intensity, which suggests that rainfall rates are increasing even if rainfall totals are not, also can be explained by the difference between thermodynamic increases in atmospheric moisture and a relatively smaller increase in total precipitation change (Trenberth 2011).

In contrast, there is substantial variability in how earth system models represent dynamic hydrological shifts (shifts in lower atmospheric currents), resulting in substantial regional variability in predictions of hydrologic variables between model projections. As climate dynamics determine how moisture-enriched air is distributed from the oceans over landmasses, shifts in circulation patterns can modify hydrologic regimes, particularly in transitional regions between human and arid climates. Variability in characterization of regional dynamic hydrologic change dominates the total uncertainty in multi-model ensemble forecasts of precipitation under climate change, an effect which is particularly apparent in transitional regions (Pfahl et al. 2017; Paxton et al. 2021; Li et al. 2024). The accuracy of regional precipitation forecasts under different global warming scenarios is therefore dependent on the physical realism of how these global models map regional precipitation anomalies to locally impactful anomalies in global and regional hydroclimatic circulation.

The Great Lakes basin spans over 1200 kilometers and straddles four climate regions in two countries: the Midwestern and Eastern climate regions of the United States, and the Northeastern Forest and Laurentian Great Lakes climate regions of Canada. The basin also occupies the transition region between the semi-arid High Plains (average annual precipitation 16-20 inches) and the humid Northeast (average annual precipitation 60-70 inches) (PRISM Climate Group 2014). The primary moisture sources for the Great Lakes basin vary spatially and seasonally, with the majority of moisture delivered as precipitation to the basin originating from the subpolar Pacific Ocean in winter months, and from the subtropical Atlantic and Gulf of Mexico in summer months (Gimeno et al. 2010; Carter et al. 2021). In the western Great Lakes, winter precipitation is generally sourced from the northern Pacific by way of polar jet stream (Rodionov 1994a, b; Rodionov and Assel 2000, 2003; Assel et al. 2004; Bai et al. 2012, 2015; Gronewold et al. 2016; Carter and Steinschneider 2018; Gronewold and Rood 2019; Carter et al. 2021). The zonal and meridional intensity of the jet stream has strong control over precipitation dynamics in the region, and dynamics of the jet stream in turn are strongly leveraged by the El Niño Southern Oscillation, with La Niña events associated with enhanced meridional activity in the jet stream and strong moist anomalies in the Northern United States and Canada. Under climate change, both El Niño and La Niña events are expected to increase in frequency and intensity, with an expected westward migration in La Niña-associated wintertime moist anomalies in the upper latitudes of North America (Trenberth and Hoar 1997; Diaz et al. 2001; Tsonis et al. 2003; Cai et al. 2014, 2015; Chen et al. 2017). This may be associated with increased interannual variability in wintertime precipitation, with a slight decline in the mean wintertime precipitation, in the Great Lakes region (McBean and Motiee 2008; Fu and Steinschneider 2019; Kayastha et al. 2022).

In the eastern Great Lakes, particularly in the warm season, precipitation variability is additionally impacted by circulation anomalies associated with the North Atlantic Subtropical High (NASH, also called the Azores High), which is a seasonally intensifying manifestation of the global Hadley circulation in the Atlantic basin (Li et al. 2011). Longitudinal thermal gradients associated with warm-season land-sea thermal contrasts in the Eastern and Western Atlantic basin cause the NASH to migrate westward during spring months, deflecting a current of moist air from the subtropical Atlantic into the continental interior, where it is convectively recycled through the eastern upper mid-Latitudes during summer months. Westerly anomalies in the NASH are associated with moist anomalies in the southeastern US and midwestern US. Under climate change, thermodynamically enhanced land-sea thermal contrasts are anticipated to be associated with a westward shift in the NASH at peak expansion, suggesting an increase in warm season Great Lakes precipitation sourced from the subtropical Atlantic (Li et al. 2011; Carter et al. 2021; Zhou et al. 2021).

1.2 Historical and future impacts of climate change on Great Lakes hydroclimatology

On top of seasonal and regional variability in oceanic moisture sources, hydroclimatic dynamics in the Great Lakes region are additionally complicated by the fact that the Great Lakes act as both a source and sink for precipitable moisture in the region. Most climate models do not parameterize lake – atmospheric climate processes, and therefore do not capture the influence of lake evaporation on precipitation formation in the region. Most models represent lakes as a static water body component of land surface or oceans, some of them do not simulate Great Lakes at all. Even models that simulate lake – atmospheric climate are limited by coarse spatial resolution relative to scale of over-lake convection/advection (Briley et al. 2021).

Understanding how Great Lakes precipitation has and will respond to shifts in regional circulation associated with climate change is challenging given the hydroclimatological complexity of the region. In the past several decades, the research community has identified substantial, complex evidence of hydrologic non-stationarity associated with anthropogenic climate change, as well as human development and lake level management (Carter and Steinschneider 2018; Fu and Steinschneider 2019; Gronewold et al. 2013). In line with expectations for thermodynamic hydrologic intensification under global warming, increases in both evapotranspiration and precipitation have been observed in the recent hydrologic record, leading to increased variability in lake levels across the Great Lakes (Held and Soden 2006; Hayhoe et al. 2010; d'Orgeville et al. 2014; Peltier et al. 2018). The main driver of extreme precipitation in the Great Lakes region is convective moisture convergence (Trenberth 1999). As the amount of moisture in the atmosphere is expected to increase with temperature, the intensity of extreme precipitation is also expected to scale with the changes of surface temperature (Pendergrass et al. 2015; Agard and Emanuel 2017; Chen et al. 2020). However, the mechanisms behind the mean rainfall response and extreme events response to warming can vary spatially. For example, current climate models predict an increase in total annual precipitation, but a drier summer in the Great Lakes region, as meteorological droughts in southwestern USA propagate eastward, reducing atmospheric moisture available for convective recycling to the Great Lakes from the High Plains region (Peltier et al. 2018; Yang et al. 2023). It is unclear whether evidence for this mechanism exists in historical record.

Uncertainties in global circulation models emerge from three different sources: internal unforced variability, model uncertainty, and radiative forcing uncertainty (Lehner et al. 2020). Among these three sources of uncertainty, model uncertainty mainly stems from structural differences among model parameterization schemes (Demory et al. 2014; Vannière et al. 2019). One of the major difficulties in precipitation projection is the coarse resolutions of earth systems models, which makes it hard to resolve mesoscale precipitation forming processes such as convective precipitation (Minallah and Steiner 2021a; Ferguglia et al. 2023). Accurate simulation of local precipitation formation processes, as well as accurate portioning the oceanic and terrestrial source of moisture that propagate seasonal precipitation anomalies, are also impacted by model spatial resolution.

1.3 Objectives

Given notable lack of agreements between numerical models in historical and future precipitation forecasts for the Great Lakes region, the goal of this analysis is to identify a subset of CMIP6 contributing model(s) which provide the most realistic depiction of dynamic drivers of Great Lakes historical precipitation variability for operational use and for selection in regional downscaling, with a focus on identifying model uncertainty arising from inaccurate parameterization of core precipitation forming processes in the region and inaccurate parameterization of regionally influential hydroclimatic dynamics. The suitability of contributing models is defined in two ways: prediction accuracy (how accurate are historical precipitation predictions?) and mechanistic accuracy (how accurately does the model identify anomalies in regional summertime hydroclimatic circulation that drive precipitation anomalies?). For evaluating mechanistic accuracy, we focus on summer months (June, July, and August) when 1) the majority of precipitation is delivered to the region, 2) the majority of precipitation is delivered by convective recycling, which is poorly parameterized in many models due to grid scale, and 3) precipitable moisture is sourced from complex circulation patterns integrating signals from the subtropical Atlantic, ENSO region, and, by teleconnection, the subpolar Pacific, underscoring the importance of accurate parameterization of hydroclimatic circulation in precipitation model accuracy. Since earth systems models (ESMs) generally show good agreement in predicting future circulation anomalies, it follows that models with higher mechanistic accuracy will likely produce better precipitation predictions under future climate scenarios.

To evaluate prediction accuracy, five indices of precipitation anomalies are calculated from historical ESM simulations and compared with observations from the same time period. To evaluate mechanistic accuracy, we quantify the non-linear correlation between summertime precipitation anomalies and characteristic anomalies in local summertime hydroclimatic circulation. The study is concluded with guidance on model selection for regional water resources managers, as well as advice for the global modeling community on selection of earth systems model for statistical downscaling, and broadly how to increase fidelity of models in this critical freshwater region.

2. Methods

2.1 Data

2.1.1 Observations of precipitation and geopotential height

The CPC Global Unified Gauge Based Analysis of Precipitation dataset, a product of the CPC Unified Precipitation Project at the NOAA Climate Prediction Center (CPC) was selected for historical precipitation validation based on availability of daily data and coverage of both Canada and the contiguous US (minimal border artifacts associated with international discrepancies of gage network maintenance and processing) (Chen et al. 2008). CPC daily precipitation is available globally from 1979-present with a grid resolution of 0.50° x 0.50°. This dataset incorporates gauge-based analysis with estimates derived from satellite observations to improve near-global precipitation analysis using Optimal Interpolation objective analysis (Chen et al. 2008).

Historical geopotential height (z) data was obtained from the NCAR/NCEP reanalysis monthly dataset, which has a resolution $2.5^{\circ} \times 2.5^{\circ}$ and historical coverage from 1948 to 2017 (Kalnay et al.1996). For each year in the study, summertime anomalies in z were calculated as the mean of the June, July, and August (JJA) monthly 500 hPa values, and were analyzed over a spatial extent of -7.50 S to 90N in latitude and 182W to 360W in longitude.

2.1.2 CMIP6 model outputs

The latest phase of the Coupled Model Intercomparison Project (CMIP), CMIP6, involves 42 modeling groups from around the world, and produced a wealth of outputs that are being used to make informed decisions about climate policy and further research in the earth's climate system (Eyring et al. 2016). Many models participating in CMIPs share common theoretical or empirical assumptions, evolve from common code banks, or developed at the same institution(s). These common model "genealogies'' represent potential sources of non-independence between models that can bias both projections and estimates of uncertainty when working with ensemble means (Steinschneider et al. 2015). To avoid functional redundancy between models, twelve models were selected that span the full range of grid resolution, equilibrium climate sensitivity, and regional transient climate representation among CMIP6 member models (Mahony et al. 2022); (Wang et al. 2016).

Table 1: CMIP6 candidate model summaries.

Model Name	Institute	Latitude	Longitude	Names Used in Paper	Reference
ACCESS-ESM1-5	Commonwealth Scientific & Industrial Research Organisation	1.25^0	1.875^0	ACCESS	*Ziehn et al (2019)*
BCC-CSM2	Beijing Climate Center	1.25^0	1.875^0	BCC	*Wu et al (2018)*
CanESM5	Canadian Centre for Climate Modelling and Analysis	2.789327^0	2.8125^0	CAN_ESM	*Swart et al(2019)*
CNRM-ESM2-1	Centre National de Recherches Météorologiques	1.400437^0	1.40625^0	CNRM_ESM	*Seferian(2018)*

EC-Earth3	EC-Earth Consortium (EC-Earth)	0.7016692^0	0.703125^0	EC_EARTH	*EC-Earth Consortium (EC-Earth) (2019)*
GFDL-ESM4	Geophysical Fluid Dynamics Laboratory/NOAA	1^0	1.25^0	GFDL	*Krasting et al(2018)*
INM-CM5-0	Institute of Numerical Mathematics	1.5^0	2^0	INM	*Volodin et al (2019)*
IPSL-CM6A-LR	Institut Pierre-Simon Laplace	1.267606^0	2.5^0	IPSL	*Boucher et al(2018)*
MIROC-ES2L	Japan Agency for Marine-Earth Science and Technology	2.789327^0	2.8125^0	MIROC	*Hajima et al(2019)*
MPI-ESM-1-2-HAM	Max-Planck-Institute fuer Meteorologie	1.864677^0	1.875^0	MPI	*Neubauer et al (2019)*
MRI-ESM2-0	Meteorological Research Institute	1.1125^0	1.1125^0	MRI	*Youkimoto et al(2019)*

Historic (1850-2014) simulations, forced by observations, are included in CMIP6 runs to allow tracking of changes in climate against change in external conditions independent from model error and bias (Eyring et al. 2016). Historical simulations of precipitation for all twelve models were accessed to assess overall prediction accuracy. Historic simulations of 500 mBar geopotential height (z500) anomalies from the five most accurate models were also extracted. These z500 anomalies are used to assess mechanistic uncertainty when characterizing the hydroclimatic dynamics in the Great Lakes region.

CMIP6 has a set of eight different emission scenarios representing different potential futures called Shared Socioeconomic Pathways (SSP). We evaluate precipitation changes in the Great Lakes region under two SSPs, SSP3-7.0 and SSP5-8.5, with radiative forcings in these scenario reach levels of 7.0 Wm^{-2} and 8.5 Wm^{-2}, respectively, at the end of the 21^{st} century in this scenario (O'Neill et al. 2016).These two scenarios, which are the highest emission scenarios in CMIP6, are used to allow for evaluation of significant response signals in the hydrologic cycle.

2.2 Data processing and analysis

2.2.1 Precipitation indices

Basin wide daily precipitation is extracted for each of the five Great Lakes basins (Lake Huron, Lake Erie, Lake Michigan, Lake Ontario, Lake Superior) from both the historical CPC and CMIP6 member datasets. To evaluate percent bias in the CMIP6 models, the mean annual total precipitation (1979-2014) and mean monthly total precipitation (1979-2014) are compared to the same values in the CPC dataset. The monthly average precipitation was compared using a nonparametric Wilcoxon test (α= 0.05) (Rey and Anselin 2010).

Daily precipitation data for each grid point of the five Great Lakes were processed into five precipitation indices to capture dry anomalies (Cumulative Dry Days), moist anomalies

(Cumulative Wet Days, Total Precipitation) and extreme precipitation anomalies (Extreme Precipitation Days, Maximum Daily Precipitation) (Table 2, (Zhang et al. 2011). All the indices were calculated for the summer season (i.e., June, July, and August), when the majority of precipitation is delivered to the region and prediction accuracy is lowest (Basile et al. 2017; Carter et al. 2021; Kunkel et al. 2022; Yang et al. 2024).

Table 2: List of Precipitation Indices

Index	Definition	Description	Unit
CDD	Cumulative Dry Days	Number of consecutive days with lower than trace amount (0.25 mm) of precipitation	Days
CWD	Cumulative Wet Days	Number of consecutive days with higher than trace amount (0.25 mm) of precipitation	Days
EPD	Extreme Precipitation Days	Number of days when the amount of daily precipitation falls above the 90^{th} percentile	Days
TP	Total Precipitation	Total amount precipitation in summer months each year	mm/year
MDP	Maximum Daily Precipitation	Maximum amount of daily precipitation each year in summer months	mm/day

2.2.2 Prediction accuracy

Dry (indicated by CDD and TP), moist (indicated by CWD and TP), and extreme (indicated by MDP and EPD) precipitation anomalies are associated with distinct circulation patterns and meteorological drivers. To evaluate the performance of CMIP6 model datasets, we evaluate how well candidate models perform in aggregate in capturing moist, dry, and extreme precipitation indices using the inter-annual variability skill score (IVSS) (Equation 1,(Srivastava et al. 2020).

$$IVSS_{m,i} = \frac{1}{N}\sum_{n=1}^{N}\left[\frac{IQR_{m,n,i}}{IQR_{o,n,i}} - \frac{IQR_{o,n,i}}{IQR_{m,n,i}}\right] \text{.....................................(Eq. 1)}$$

Here, *IQR* is the interquartile range for an index *i* at location *n*, between a modeled dataset *m* and observed dataset *o*, where *N* is the total number of grid points in the dataset. A perfectly simulated model will have an IVSS value of zero, the larger the IVSS, the poorer the performance of the model. To compare the relative performance of the model relative to other CMIP6 models, calculate the normalized interannual variability score (NIVSS, Equation 2, (Srivastava et al. 2020).

$$NIVSS_{m,i} = \frac{IVSS_{m,i} - IVSS_{CMIP6,median}}{IVSS_{CMIP6,median}} \text{.......................................(2)}$$

Here, $IVSS_{CMIP6,median}$ is the median IVSS of index *i* across all twelve candidate CMIP6 models. A negative NIVSS value indicates that the model is performing better than most of the other models and a positive value indicates decreasing skill. This metric of comparing models based on NIVSS is known as evaluating the Model Variability Index (MVI). MVI is the median across all indices of a models NIVSS values. Models with a MVI value less than zero are considered the best performing models (Chen et al. 2011; Jiang et al. 2015; Srivastava et al. 2020).

For calculating performance metrics (NIVSS and MVI, Equations 1 and 2), precipitation indices were calculated for each grid at original model resolution. For comparison, the observed precipitation dataset (CPC) was resampled by the nearest neighbor method to each model resolution (Table 2).

2.2.3 Dynamic accuracy

Rank correlation between observed and modeled total precipitation (TP) and denoised geopotential height anomalies is used to identify dominant spatiotemporal circulation patterns associated with anomalous precipitation in both observed (NCAR/NCEP) and the high-performing models in the CMIP6 dataset (Section 2.2.2). Using the method of Yin (2018), for each dataset, the minimum number of principal components that explained at least 75% of the variance in the total dataset are selected, and their loadings are combined and inverted back into the original dimension to denoise the data. Spearman rank correlation between these gridded denoised z500 and yearly precipitation anomalies are calculated for each grid cell in the spatial field of z500. Correlation coefficients which exclude zero with a 90% confidence interval are considered significant. The spatial variability in the magnitude of Spearman's correlation coefficient helps us to identify atmospheric regions where modelled and observed circulation anomalies translate to anomalies in Great Lakes precipitation. The modeled and observed spatial correlation patterns are compared. This information, which indicates fidelity of the model in capturing dynamical drivers of hydroclimatic variability in the region (“dynamic accuracy”), is then used to assist in the interpretation of the fidelity of future precipitation forecasts.

2.3 Forecasted trends in precipitation indices

Five models are selected based on their historic performance, as indicated by MVI values and dynamic accuracy, to evaluate future projections of summertime (JJA) precipitation indices. Significant trends are identified through a Mann-Kendall trend test (α=0.05), and ordinary least squares regression is used to quantify the magnitude of 21st century trends in historically mean-centered JJA precipitation indices (i.e. with the historical (1974-2014) mean of each precipitation index for each individual models forced to the y-intercept). This was used to infer the magnitude of projected 21st century changes in precipitation indices.

3. Results

3.1 Historical accuracy

Almost all candidate models show a consistent positive bias in annual total precipitation (TP) estimates across the Great Lakes basin (Figure 1), a trend that intensifies moving from the western to eastern reach of the basin (Fig 2a). GFDL shows the strongest overall positive bias, with 44.22% overestimation of annual TP relative to CPC data, followed by ACCESS (41.03%), MIP (39.71%), MRI (39.23%), and CAN_ESM (36.91%) and EC_EARTH (35.58%). While TP is largely overestimated by all the models (Figure 2c), both EPD and CWD show comparatively little bias (Figure 2b, 2d). In contrast, a strong positive bias in MDP, with a negative variance bias and strong intermodal agreement, is seen (Figure 2e). On an annual basis, CDD shows minimal mean bias, but negative variance bias and strong intermodal agreement (Fig 2a).

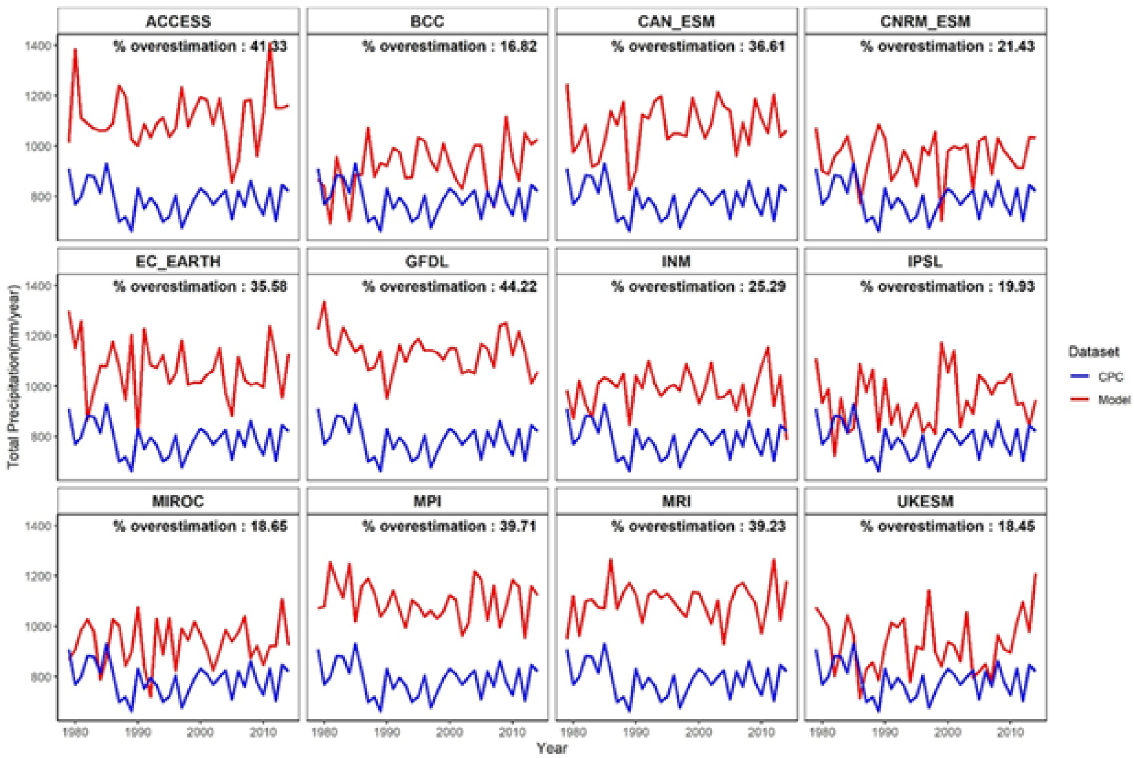

Figure 1. Annual Total Precipitation (TP) in 12 participating models and CPC dataset

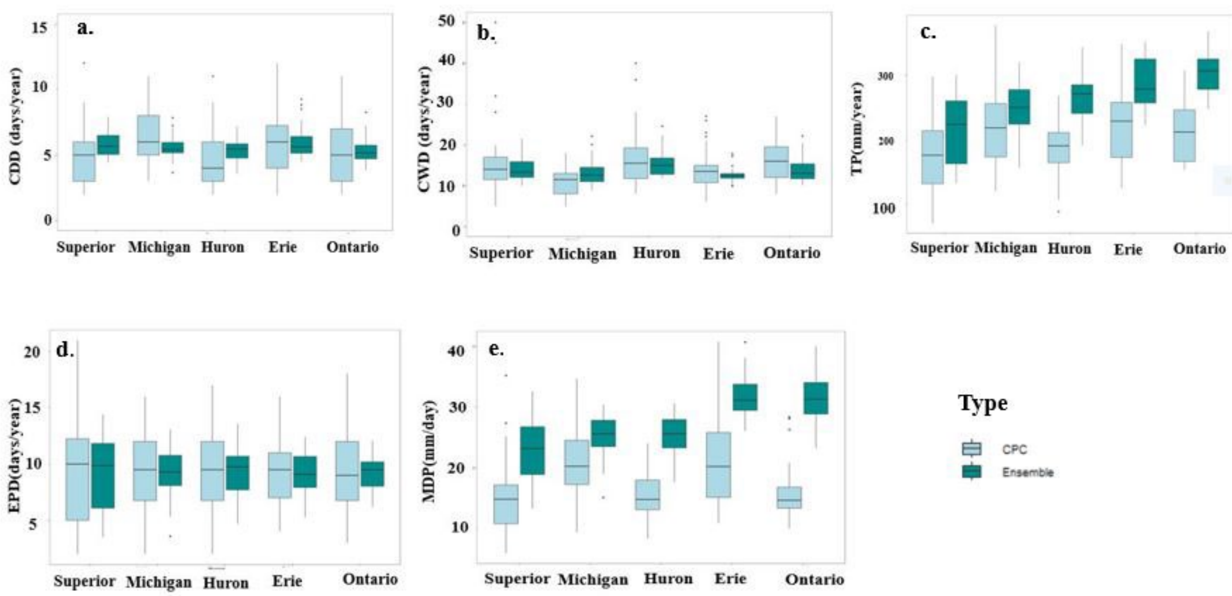

Figure 2. Annual CDD, CWD, TP, EPD and MDP by lake basins in 12-model ensemble mean and in CPC dataset. The solid line inside each box represents the median value, the box area represents the inter-quartile range; the upper and lower whisker respectively represent the upper and lower 25th percentile. The lake basins are organized west to east to aid the interpretation

Based on CPC observations, February is on average the driest month in the Great Lakes Basin, and June-September has the most TP (Fig 3). Models that show some fidelity in capturing seasonal trends tend to do so in winter or early spring months (ACCESS, BCC, CNRM, EC_EARTH, GFDL, INM, MIROC, MPI, MRI). Fewer models capture the observed trend of precipitation increasing from March to June, stabilizing at this high until August, before declining from September to December (CNRM, GFDL, MIROC, MPI, MRI). All models demonstrate significant positive or negative bias in some monthly precipitation estimates. Consistent with the bias observed in annual precipitation predictions, a positive or wet bias is observed in most models during most months, but particularly in the spring months (March, April, May). In addition to mean bias in monthly precipitation, models show greater interannual variability in monthly precipitation than CPC data, suggesting an overestimation of monthly precipitation variance (Fig 3).

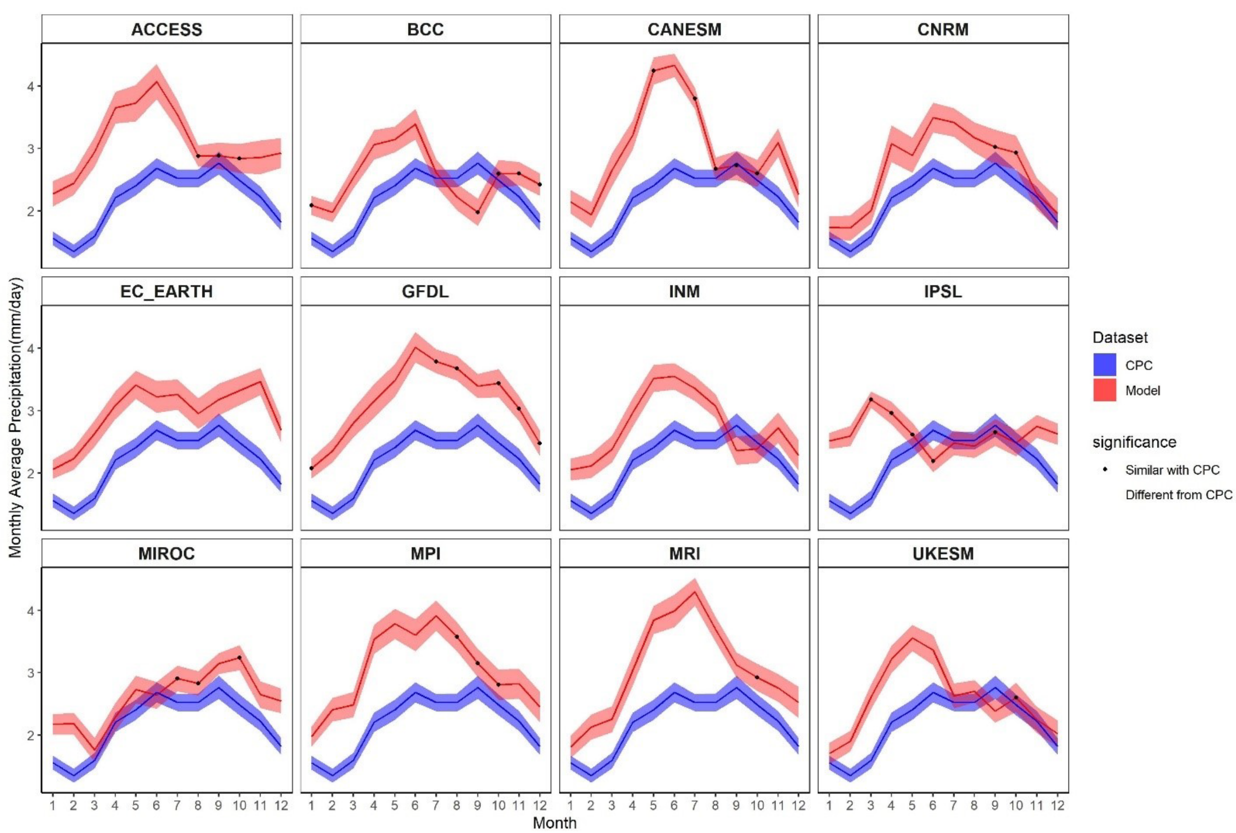

Figure 3. Average monthly precipitation for 12 CMIP6 models (red) and CPC observations (blue) with standard error. Stippling indicates no statistically significant difference between observed and modelled monthly mean precipitation.

The overall model performance across all precipitation indices is integrated into the model variability index (MVI), which is the median of the interannual variability skill scores (IVSSs) over all indices for that model (Fig 4, top row). A model with a negative MVI value is considered to have higher accuracy relative to other models. The normalized interannual variability skill score (NIVSS), which is an indicator of relative model performance in capturing a historical precipitation index, is calculated by normalizing the respective IVSS with respect to the median IVSS over all candidate models. The relatively well performing models across all precipitation indices, as indicated by negative MVI values, are EC-Earth, MPI, MRI, ACCESS and MIROC (Fig 4). These five models were used to examine the trends in future precipitation indices.

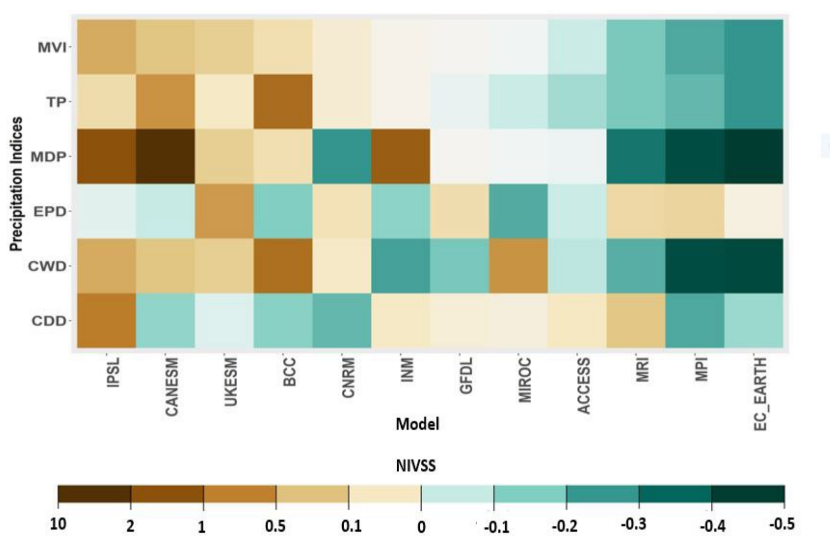

Figure 4. Portrait diagram of normalized IVSS over the 1979-2014 period. Model MVI is shown in the top row, which is the median of IVSSs over all indices for that model.

The higher performing models, EC_Earth and MPI, which had the first and second ranking MVI respectively, consistently showed good agreement in inter-annual measurements of moist anomalies (TP, MDP, CWD) and dry anomalies (CDD). Neither model showed relative skill in capturing historic distributions of EPD. MRI (the third ranking model) had comparable performance in capturing EPD as EC_Earth and MPI. Like MRI, ACCESS and MIROC (the fourth and fifth ranking MVI models, respectively) did not perform well relative to other candidate models in predicting dry anomalies (CDD), but performed well in capturing EPD. Similarly, several models with less accuracy in predicting moist anomalies (CNRM and CANESM) were more effective in predicting CDD (Fig 4).

3.2 Model mechanistic accuracy

Only the top five ranking MVI models were selected for geopotential height analysis: EC_Earth, MPI, MIR, ACCESS, and MIROC. In the historical observations, we see that TP in the Great Lakes region is correlated with a z500 anomaly tripole that spans the northeast hemisphere mid-latitude region, with positive (negative) TP associated with a positive (negative) z anomaly over the Gulf of Alaska, a negative (positive) z anomaly over central/eastern Canada, and a positive (negative) z anomaly over the Labrador Sea. We also see a significant correlation between summer Great Lakes TP and the Gulf of Mexico/southeastern United States, with positive (negative) summertime TP associated with positive (negative) z500 in the region (Fig 5a).

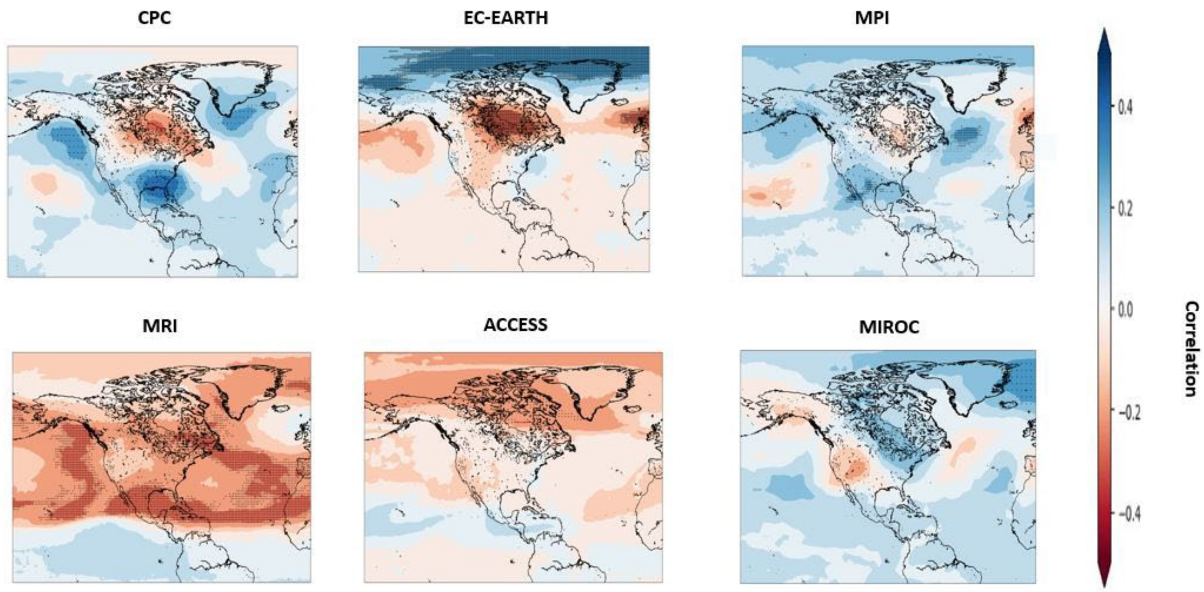

Figure 5. Correlation between denoised z500 mb and Great Lakes summer (JJA) total precipitation (TP).

The two models which come closest to replicating the midlatitude z500 tripole pattern associated with increased Great Lakes summer TP are EC_EARTH and MPI, which were also the top two ranking models based on MVI. Both EC_Earth (Figure 5b) and MPI (Figure 5c) capture a positive-negative-positive correlation at approximately the same longitude as what is seen approximately the focal regions of the Pacific North Atlantic oscillation pattern in observations (Fig 5a). In EC_Earth (Fig 5b), the positive regions of this tripole are shifted about 20° north. In MPI (Fig 5c), the negative region of the tripole has a locus in approximately the same geographic location as is captured in observations, but correlations between TP and z500 in this region are not statistically significant. The only model to capture a significant z500 anomaly in the subtropical Atlantic region is MPI. Both ACCESS and MRI, the third and fourth ranking models by MVI, show little to no fidelity to observed correlation between z500 and summertime TP. In ACCESS, extremely limited statistically significant correlation is observed between modeled TP and any z500 anomalies in the northeastern hemisphere (Fig 5d). In MRI, modeled TP is broadly negatively correlated with increased z500 across the northeastern hemisphere, bearing little resemblance to the observed patterns (Fig 5e). MIROC, the fifth ranking model for MVI but the highest-ranking model for CDD, captures a weak mid-latitude tripole linking z500 to modeled TP, but it is in the wrong phase over North America. MIROC approximately captures the observed correlation between z500 and TP well over the Labrador Sea (Figure 5f).

3.3 Future precipitation predictions

Of the top five ranking models by MVI, only the first two ranking (MPI and EC_Earth) had negative IVSS scores for CDD. These models returned diverging low magnitude, though statistically significant (at SSP 3-7.0 and SSP5-8.5 for EC_EARTH, and at SSP5-8.5 only for MPI) trends for future CDD. EC_Earth predicts an increase in summertime maximum CDD of between 1.0-1.2 days/year by 2100 (for SSP3-7.0 and SSP5-8.5, respectively). MPI suggests an increase in summertime maximum CDD of 0.9 days/season by 2100 (for SSP5-8.5 only) (Fig 6). Statistically significant increases in CDD are projected in MRI and ACCESS as well (corresponding to 0.7 to 1.2 days/ season by 2100). No significant trends are observed in MIROC.

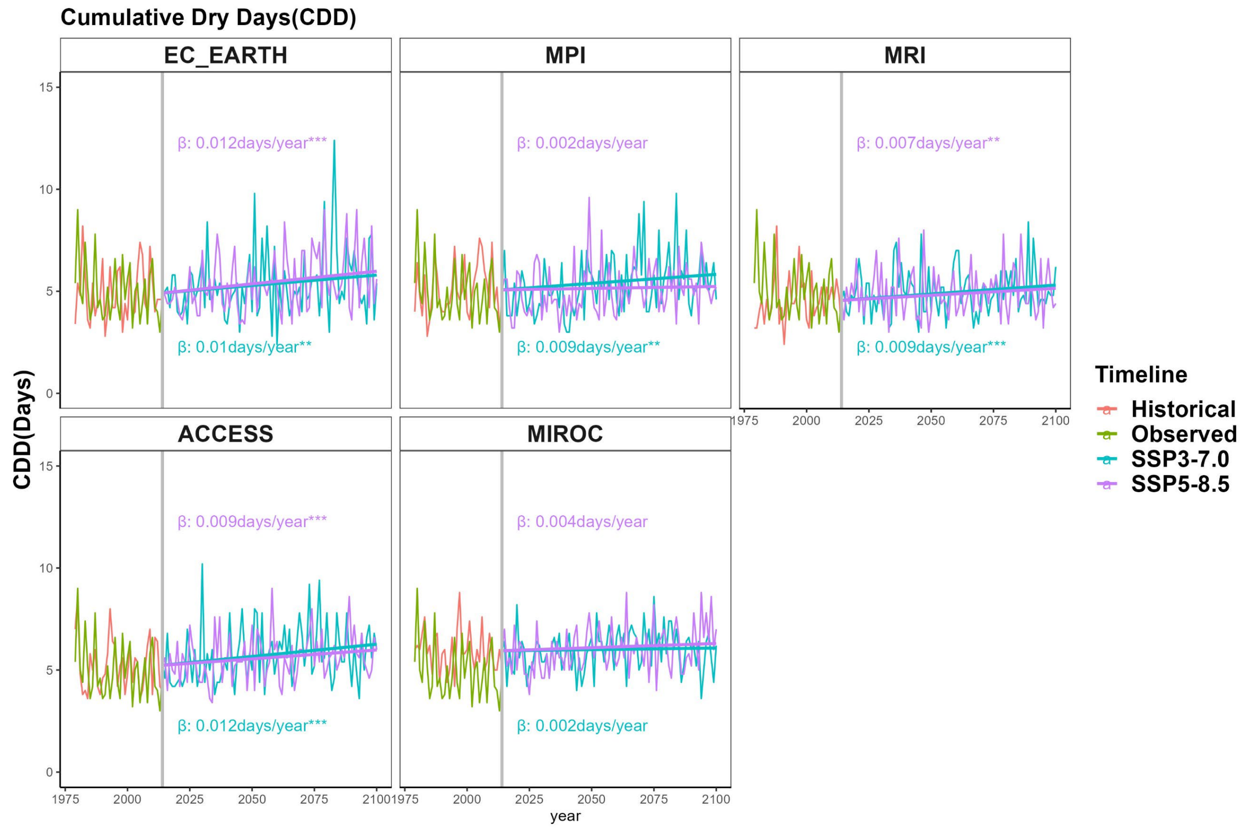

Figure 6. Historic (1974-2014) modelled and observed CDD, and projected (2015-2100) CDD under SSP3-7.0 and SSP5-8.5, with future OLS trendlines.

In historical simulations, MRI, MPI, and EC-Earth showed the greatest still in capturing interannual variability in CWD (Figure 7), yet there is little consensus between these models on future trends in cumulative wet days. MPI is the only model projecting significant trends in CWD under both SSP pathways, corresponding a decrease of between 1.7 and 2.4 days in a wet day sequence by 2100. MIROC predicts a statistically significant increase corresponding to about 1.2 days per wet sequence per season by 2100 for SSP5-8.5 only; this trend is not conserved by SSP3-7.0.

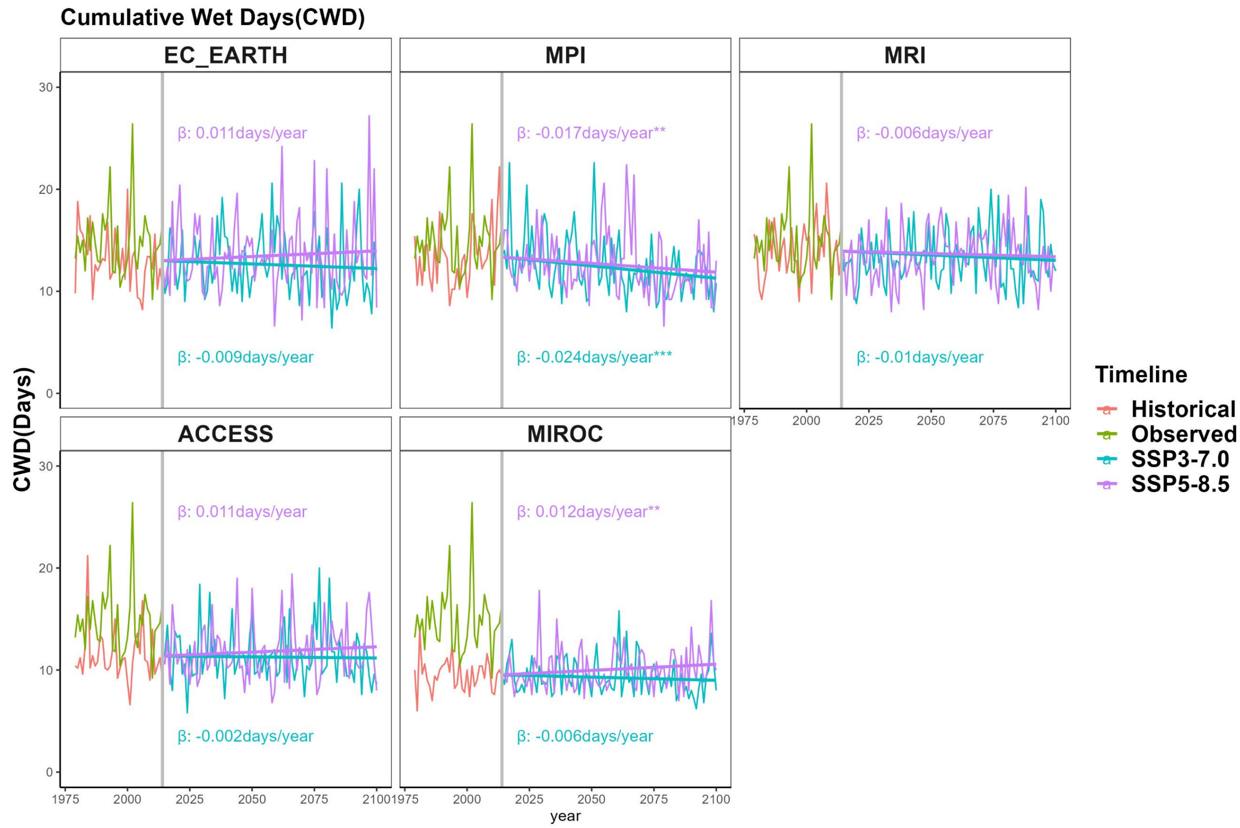

Figure 7. Historic (1974-2014) modelled and observed CWD, and projected (2015-2100) CWD under SSP3-7.0 and SSP5-8.5, with future OLS trendlines.

Extreme precipitation days (EPD) is an index of storm duration. MIROC and ACCESS, the two models which performed best relative to other candidate models amongst the top-five ranking MVI models in predicting EPD, showed significant negative trends in the 21st century, corresponding to an decrease in EPD of 0.2 to 0.8 days/season by 2100. EC_Earth and MRI, which were the top-performing models overall in terms of prediction and mechanistic accuracy, also indicate weak but contrasting 21st century trends in EPD, corresponding to an decrease in EPD of 0.3 to 0.7 days/season by 2100. No significant trends in EPD are projected by MRI (Fig 8).

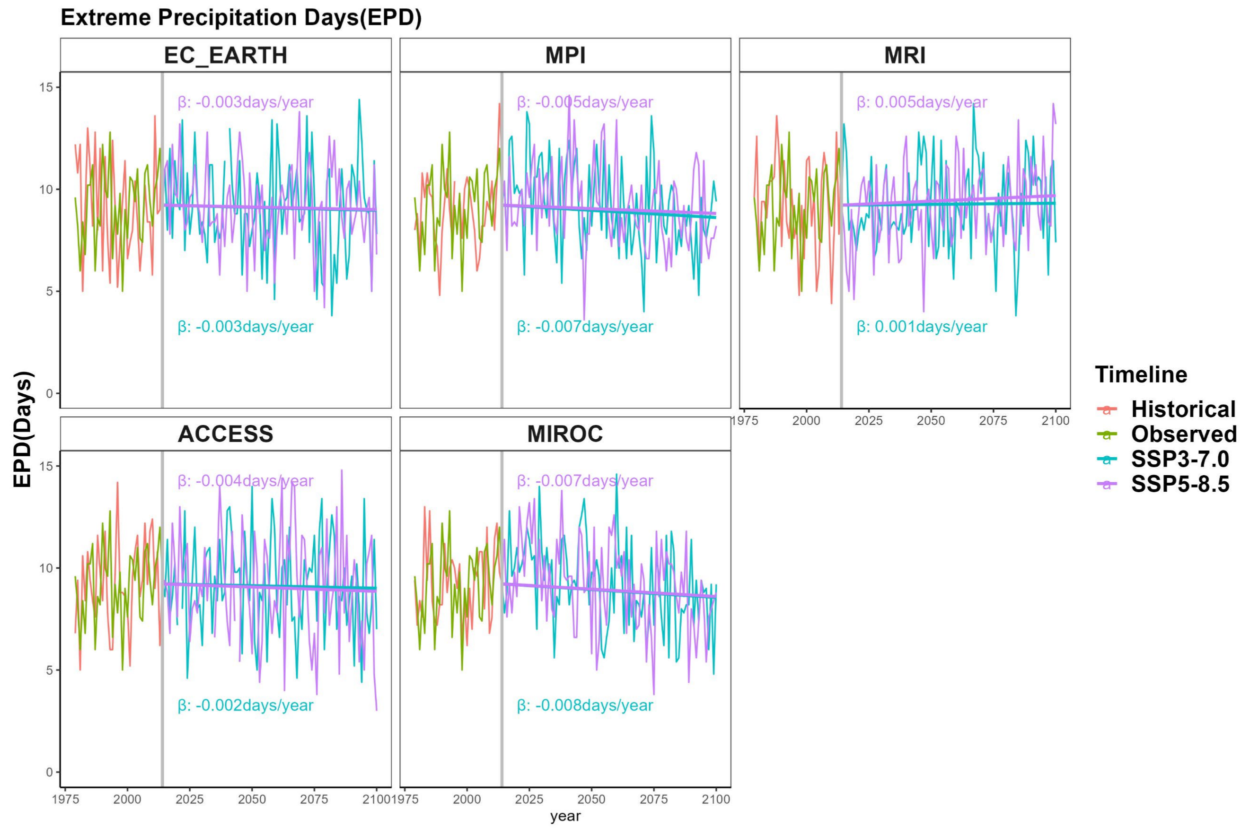

Figure 8. Historic (1974-2014) modelled and observed EPD, and projected (2015-2100) EPD under SSP3-7.0 and SSP5-8.5, with future OLS trendlines.

Maximum daily precipitation (MDP) is an indicator of storm intensity. The models are split in the direction of future trends. EC_EARTH, MRI (two of the models with lowest NVISS for MDP) and MIROC all suggest significantly increasing MDP by 2100; under both emission scenarios for EC_EARTH and MRI, and under SSP5-8.5 only for MIROC. ACCESS, in contrast, projects a significant negative trend in MDP under both SSPs. MPI, which had the second lowest NIVSS for historical MDP, projects no trends in MDP under either SSP (Fig 8).

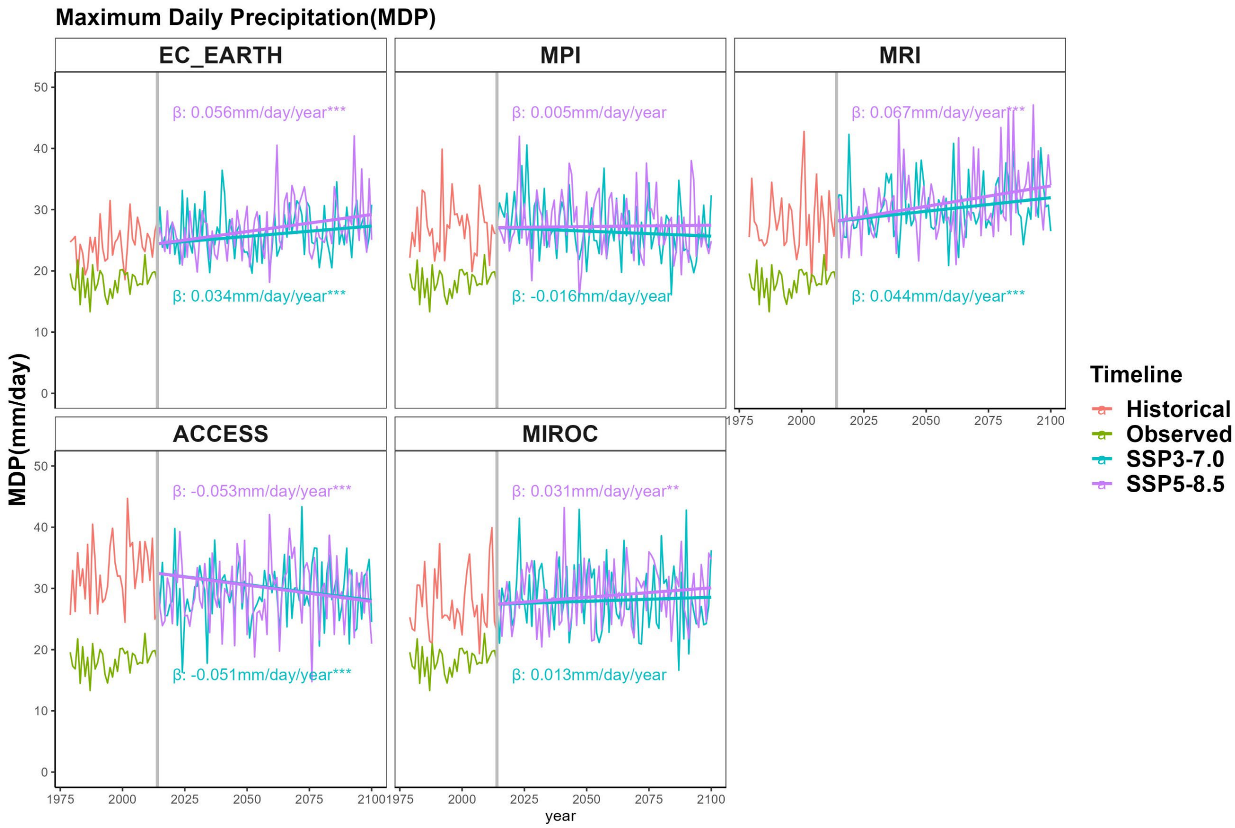

Figure 9. Historic (1974-2014) modelled and observed MDP, and projected (2015-2100) MDP under SSP3-7.0 and SSP5-8.5, with future OLS trendlines.

Models likewise diverge on summertime total precipitation (TP) anomalies, an index of anomalous atmospheric dynamics. EC_EARTH, ACESS, and MIROC all project decreases in summertime TP, ranging from 13.7 to 88.0 mm per season by 2100. MPI and MRI project statistically significant increases in summertime TP, ranging from 23.3-58.2 mm per season by 2100, but for SSP5-8.5 only. No significant trends are seen in summertime TP in these models under SSP3-7.0 (Fig 9).

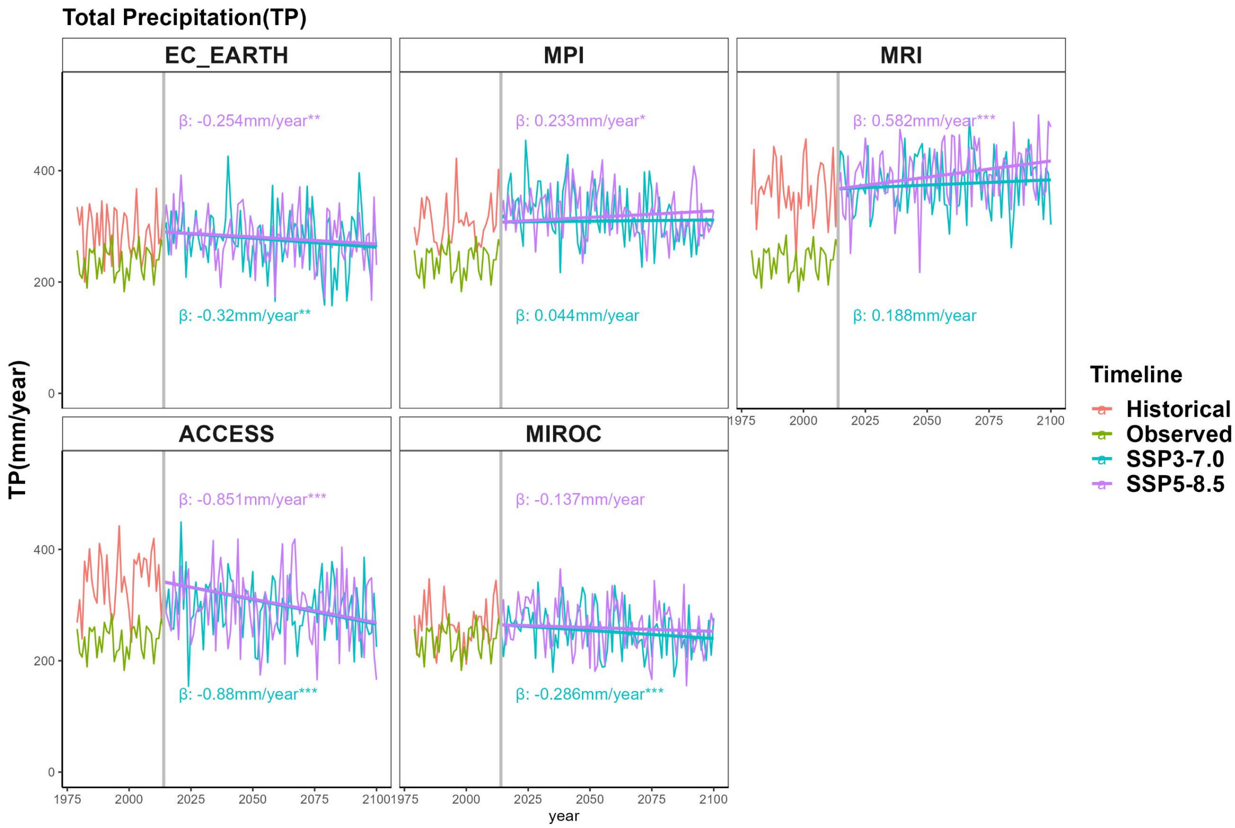

Figure 10. Historic (1974-2014) modelled and observed TP and projected (2015-2100) TP under SSP3-7.0 and SSP5-8.5, with future OLS trendlines.

4. Discussion

General circulation models participating in CMIP experiments have shown notoriously low fidelity in capturing hydrometeorological and hydroclimatic variability in the Midwestern and Northeastern United States (Akinsanola et al. 2020); (Minallah and Steiner 2021b), particularly during summer months (Peltier et al, 2018). This limits effective planning for water resources management in the Great Lakes basin, which contains over 25% of global freshwater resources. This analysis investigates how twelve models capturing a wide range of climate parameterizations participating in the latest CMIP experiment, CMIP6, perform in capturing several different indices of summertime extreme dry, moist, and wet precipitation in the Great Lakes region. By examining the accuracy and precision of models in capturing the historical distribution of these precipitation indices (CWD, CDD, EPD, MDP, and TP), the performance of models in capturing different mechanisms of precipitation delivery are explored. As future hydroclimatic shifts will be associated with by thermodynamic intensification of the hydrologic cycle as well as dynamical shifts in integrated vapor transport, we additionally hypothesize that model hydroclimatic fidelity will be related to its accuracy in capturing relationships between precipitation anomalies and circulation anomalies in regional hydroclimatic circulation, as indicated by correlation between geopotential height and seasonal anomalies in total precipitation. Uncertainties in CMIP6 model predictions are associated with both internal variability and model uncertainty. These model uncertainties, which can be observed as biases in historical simulations and inconsistencies in the relationship between precipitation anomalies in hydroclimatic circulation anomalies, will likely be conveyed in future projections (John et al. 2022). We thus seek to identify models with the greatest physical realism in capturing the regional hydroclimatic system to guide our interpretation of diverging predictions of future hydroclimate scenarios.

The 5th Assessment Report of Intergovernmental Panel on Climate Change (IPCC) uses two metrics to identify the fidelity of GCM model performance to external forcings: the Equilibrium Climate Sensitivity (ECS), which evaluates the models' long term rebound to climatological stasis after an instantaneous doubling of atmospheric CO2, and the Transient Climate Response (TCR), which evaluates the models' projected equilibrium response to an incremental increase in atmospheric CO2 (Tokarska et al. 2020; Nijsse et al. 2020). The five models identified as higher performing in the Great Lakes region based on IVSS (EC_Earth, MPI, MRI, ACCESS, and

MIROC) all have ECS and TCR values identified in the range of "likely warming" by the IPCC, building confidence in our findings.

Almost all candidate models show a consistent positive bias (17-44% depending on the model) in annual total precipitation estimates relative to CPC precipitation (Fig 1). The positive bias in total precipitation grows stronger as we move from west to east across the basin (Fig 2). A climatological increase in precipitation that is stronger on the eastern range of the Great Lakes basin could be associated with increased flood risk on the eastern edge of the basin, which integrates anomalous runoff across all the upper Great Lakes before it is discharge to the Atlantic by way of the Saint Lawrence Seaway. Individual GCM's bias towards overestimation of annual precipitation has been identified in the literature (Li et al. 2014).

Consistent model biases in climatological precipitation show seasonal patterns as well, with weak agreement observed between modeled and actual precipitation in fall/winter months for most models (MRI, ACCESS, MIROC, UKESM, INM, MPI, BCC, Can-ESM, and CNRM_ESM), and limited to no skill seen in capturing the monthly distribution of precipitation during the warm season (Fig 3). The relative accuracy of cold season model predictions has been observed in the literature, and is likely attributable to the fact that winter precipitation anomalies are strongly leveraged by regional teleconnection patterns, particularly the El Niño Southern Oscillation (ENSO) and the Pacific North American pattern (PNA). Summertime circulation anomalies are associated with small scale convective process (Li et al. 2011) and lesser-characterized, more volatile modes of anomalous large scale circulation, such as dynamics associated with the propagation and decay of the southwestern ridge under the summertime peak of the North Atlantic Subtropical High (W. Li et al. 2011, Zorzetto and Li 2021). As the majority of precipitation to the Great Lakes basin is delivered during summer months and hydroclimatic dynamics in the region are most complex during this time, we make the accuracy of warm season precipitation the primary focus of our study.

The primary mechanism of precipitation delivery in the summertime in the Great Lakes region is the convective recycling of moisture sourced from the subtropical Atlantic and, to a lesser extent, northern Pacific (Gimeno et al. 2010). This Atlantic-sourced moisture travels upward into the continental interior through convective recycling, following the western ridge of the North Atlantic subtropical high (NASH) in the southern mid-latitudes, and then travels eastward along with the Pacific-moisture enriched jet stream in the northern mid-latitudes. Positive anomalies in meridional integrated vapor transport along the western ridge of the NASH have been related to increased precipitation intensity in the eastern United States in the last century (Li et al. 2011; Carter et al. 2021; Zorzetto and Li 2021; Teale and Robinson 2022). The mid-latitude tripole observed in spatial correlations between geopotential height (z500) and TP in Fig 6 mirrors these past results, and closely resembles the PNA (Wallace and Gutzler 1981), confirming that a negative phase of the PNA is associated with increased summertime precipitation in the region (Andresen et al. 2012; Malloy and Kirtman 2020). In addition, a strong positive relationship is seen between TP and increased z500 in the region corresponding with the climatological summer westward position of the NASH confirms that increased NASH intensity is associated with enhanced integrated vapor transport, and associated increases in convective precipitation, throughout the central and eastern United States (Fig 6, Wang et al. 2007; Li et al. 2011; Bishop et al. 2019; Zhou et al. 2021; Zorzetto and Li 2021).

Overestimation of wet indices may stem from the "drizzle problem" in general circulation models, where low frequency, high intensity precipitation is overestimated, but persistent low-intensity precipitation is underestimated (Gibson et al. 2019);(Dai and Trenberth 2004). While TP is largely overestimated by all models, both EPD and CWD show comparatively little bias (Fig 2, Fig S9 and Fig S6) suggesting that origin of consistent overestimation in TP in this region is not associated with inaccuracy in parameterizations related to frequency and duration of precipitation events, but in rainfall intensity. In addition, our analysis shows strong positive bias in MDP across the Great Lakes basin, with a negative variance bias and strong inter-model agreement (Fig 2, S6, S9, and S15). Convective storms occur on the scale of meters to kilometers and, as such, are not well parameterized in most CMIP6 models which run on a grid scale of hundreds of kilometers or greater (Li et al, 2010; (Cristiano and Veldhuis 2017). As positive moisture anomalies in TP can result from either short duration high intensity storms, or long duration low intensity storms, our patterns indicate that MDP and CWD are contributing less to overestimate of TP than EPD, suggest that "drizzle bias" persists in CMIP6 models in the region.

This work that resolution of models may not have as much effect on finding statistical similarities in precipitation characteristics as it was supposed. Of the selected models, EC_earth and MPI showed the highest accuracy in capturing historic distributions of MDP (Fig 4). Both of these models demonstrated correlation patterns between TP anomalies and z500 anomalies in the subtropical north Atlantic that most nearly match historic observations (Fig 5). ACCESS and MIROC showed the poorest performance in capturing historical MDP (Fig 4), and likewise showed no significant spatial correlation between TP anomalies and z500 anomalies in the subtropical North Atlantic (Fig 5). This is consistent with under-parameterization of meridional integrated vapor transport associated with convective recycling of Atlantic-sourced moisture, which has shown an increasing relationship with precipitation intensity in the eastern United States in the last century (Teale and Robinson 2022), and further suggests that parameterization of the relationship between geopotential height anomalies and integrated vapor transport anomalies throughout the continental interior, as well as more accurate parameterization of the magnitude and variance of convectively recycled warm season extreme precipitation, are essential components of capturing current and future climatological precipitation in the Great Lakes region.

Evaluating future hydroclimate from the perspective of accurate climate models indicate that we may expect to see a slightly drier summer in the Great Lakes region, corresponding to an 13.7 to 88.0 mm decrease in summertime TP, which is consistent with results from other studies in Midwestern and Northeastern US (Zhou, Ruby Leung, and Lu 2022; Richard Peltier et al. 2018; Akinsanola et al. 2020). The slight decrease in TP appears to be largely driven by significant increases in CDD, corresponding to a 0.9 to 1.2 increase in dry days per longest dry spell per year. Decrease in storm duration (CWD) and increase in dry periods (CDD), are historically associated with a strong ridge over the central United States, which weakens the storm track in the midwestern region and causes blocking in the late summer season (Chen et al, 2022). Less frequent or persistent precipitation may also be driven by a dynamic reduction in atmospheric moisture content in this region in the months of July and August, defined by a eastward shift in aridity associated with enhanced land-sea thermal contrast in the region (Mailhot et al. 2019;

Minallah and Steiner 2021). Similar trends are also found in Akinsanola et al. (2020) and Dollan et al. (2022).

We see skillful and dynamically precise models diverging in projects of maximum daily precipitation (MDP), our major indicator of thermodynamic intensification of the climate indices. We observe that higher spatial resolution models (EC_EARTH at 0.7° resolution, MRI at 1.1° resolution) predict increases in MDP, whereas our lower resolution models (MPI at 1.9° resolution, ACCESS at 1.25° resolution, and MIROC at 2.8° resolution) predict slightly increasing to neutral to strongly decreasing tends in MDP (Table 2). As convective storms tend to be shorter in duration and higher in intensity, this trend is consistent with gains in convective precipitation prediction seen in higher resolution models. Increases in in MDP in humid regions and increases in CDD in arid regions clearly mirroring the "wet gets wetter"' characterization of thermodynamic intensification of the hydrologic cycle under climate change (Li et al. 2021). Signatures of thermodynamic intensification were also found in CMIP5 higher emission scenarios (Shrestha et al. 2022). In particular, observed intermodal disparities in MDP predictions may indicate differences in model parameterizations of dynamical shifts under climate change, where slight changes in geopotential height patterns the transitional Great Lakes region could modify the spatial distribution of integrated vapor transport, and thus modify the spatial distribution of moisture and energy limited hydroclimatological regimes within the region.

As this strong intermodal positive bias in TP appears to be associated with a negative "drizzle bias," or overprediction of intense precipitation events at the expense of long-duration low-intensity events, confidence in future prediction of increased intense precipitation is degraded. These results contribute information, if not insight, into the debate about the efficacy bias correction in future precipitation predictions in the Great Lakes region (Ehret et al. 2012). Four of our five selected models predicted an increase in the dry index (CDD). This signal indicates consensus on increased risk for meteorological drought in the region.

5. Conclusion

The goal of this study was to identify which models demonstrate the most physical fidelity in capturing circulation anomalies related to seasonal and climatological variability in Great Lakes precipitation. Physically realistic models are most likely to make accurate future predictions, which is important for policy planning to mitigate the effects of a changing climate in this critical freshwater region. Relative performance of models against observed precipitation was assessed using NOAA CPC unified gauge adjusted dataset. Model Variability Index (MVI) was calculated to compare the distributions of historical and modelled precipitation indices. Models selected on the basis of MVI values were used to estimate the trends in future precipitation in two different emission scenarios.

In terms of large circulation patterns, the highest two performing models both capture a PNA-like pattern seen in observations over in the mid-latitude region, and one (MRI) captures a relationship between enhanced TP and intensification of the North Atlantic subtropical high, lending confidence in their predictions. Accurate representation of these hydroclimatic circulation patterns are associated with greater skill in capturing warm-season distribution of convectively recycled precipitation in the region. Models chosen based on their overall skill score in historic precipitation variability in the Great Lakes region predict a drier summer, where longer dry spells and shorter duration precipitation are largely balanced out by an increase in precipitation intensity in those events.

Acknowledgements:

NCEP reanalysis data were provided by the NOAA/OAR/ESRL PSD, Boulder, Colorado, USA, from their website at https://www.esrl.noaa.gov/psd/. TM received financial support from the Syracuse University Graduate Fellowship program. EC is supported by the United States Geological Survey Grant 170655-23048 and received financial support from the United States Geological Survey New York State Water Resources Institute/New York State Water Science Center. TB is supported by National Science Foundation P4Climate Program Grant AGS-2402498, and by Sloan Foundation Fellowship FG-2023-20259.

References

Agard V, Emanuel K (2017) Clausius-Clapeyron scaling of peak CAPE in continental convective storm environments. J Atmos Sci 74:3043–3054

Akinsanola AA, Kooperman GJ, Reed KA, et al (2020) Projected changes in seasonal precipitation extremes over the United States in CMIP6 simulations. Environ Res Lett 15:104078

Allan RP, Barlow M, Byrne MP, et al (2020) Advances in understanding large-scale responses of the water cycle to climate change. Ann N Y Acad Sci 1472:49–75

Allen MR, Ingram WJ (2002) Constraints on future changes in climate and the hydrologic cycle. Nature 419:224–232

Andresen J, Hilberg S, Kunkel K, Center MRC (2012) Historical climate and climate trends in the Midwestern USA. US National Climate Assessment Midwest Technical Input Report 1–18

Assel RA, Quinn FH, Sellinger CE (2004) Hydroclimatic factors of the recent record drop in Laurentian great lakes water levels. Bull Am Meteorol Soc 85:1143–1152

Bai X, Wang J, Austin J, et al (2015) A record-breaking low ice cover over the Great Lakes during winter 2011/2012: combined effects of a strong positive NAO and La Niña. Clim Dyn 44:1187–1213

Bai X, Wang J, Sellinger C, et al (2012) Interannual variability of Great Lakes ice cover and its relationship to NAO and ENSO. J Geophys Res C: Oceans 117:. https://doi.org/10.1029/2010JC006932

Basile SJ, Rauscher SA, Steiner AL (2017) Projected precipitation changes within the Great Lakes and Western Lake Erie Basin: a multi-model analysis of intensity and seasonality. Int J Climatol 37:4864–4879

Bishop DA, Williams AP, Seager R, et al (2019) Investigating the causes of increased twentieth-century fall precipitation over the southeastern United States. J Clim 32:575–590

Briley LJ, Rood RB, Notaro M (2021) Large lakes in climate models: A Great Lakes case study on the usability of CMIP5. J Great Lakes Res 47:405–418

Cai W, Borlace S, Lengaigne M, et al (2014) Increasing frequency of extreme El Niño events due to greenhouse warming. Nat Clim Chang 4:111–116

Cai W, Santoso A, Wang G, et al (2015) ENSO and greenhouse warming. Nat Clim Chang 5:849–859

Carter E, Herrera D, Steinschneider S (2021) Feature engineering for subseasonal-to-seasonal warm-season precipitation forecasts in the Midwestern United States: Toward a unifying hypothesis of anomalous warm-season hydroclimatic circulation in the Midwestner US. Journal of Climate 34:8291–8318

Carter E, Steinschneider S (2018) Hydroclimatological drivers of extreme floods on Lake Ontario. Water Resour Res 54:4461–4478

Chen C, Cane M, Wittenberg A, Chen D (2017) ENSO in the CMIP5 simulations: Life cycles, diversity, and responses to climate change. Journal of Climate 30:775–801

Chen J, Dai A, Zhang Y, Rasmussen KL (2020) Changes in convective available potential energy and convective inhibition under global warming. J Clim 33:2025–2050

Chen W, Jiang Z, Li L (2011) Probabilistic projections of climate change over China under the SRES A1B scenario using 28 AOGCMs. J Clim 24:4741–4756

Cristiano, Veldhuis (2017) Spatial and temporal variability of rainfall and their effects on hydrological response in urban areas–a review. Hydrol Earth Syst Sci

d'Orgeville M, Peltier WR, Erler AR, Gula J (2014) Climate change impacts on Great Lakes Basin precipitation extremes. J Geophys Res 119:10,799-10,812

Dai A, Trenberth KE (2004) The diurnal cycle and its depiction in the community climate system model. J Clim 17:930–951

Demory M-E, Vidale PL, Roberts MJ, et al (2014) The role of horizontal resolution in simulating drivers of the global hydrological cycle. Clim Dyn 42:2201–2225

Diaz HF, Hoerling MP, Eischeid JK (2001) ENSO variability, teleconnections and climate change. Int J Climatol 21:1845–1862

Ehret U, Zehe E, Wulfmeyer V, et al (2012) HESS Opinions "Should we apply bias correction to global and regional climate model data?" Hydrol Earth Syst Sci 16:3391–3404

Eyring V, Bony S, Meehl GA, et al (2016) Overview of the Coupled Model Intercomparison Project Phase 6 (CMIP6) experimental design and organization. Geosci Model Dev 9:1937–1958

Ferguglia O, von Hardenberg J, Palazzi E (2023) Robustness of precipitation Emergent Constraints in CMIP6 models. Clim Dyn 61:1439–1450

Fu W, Steinschneider S (2019) A diagnostic-predictive assessment of winter precipitation over the Laurentian Great Lakes: Effects of ENSO and other teleconnections. J Hydrometeorol 20:117–137

Gibson PB, Waliser DE, Lee H, et al (2019) Climate model evaluation in the presence of observational uncertainty: Precipitation indices over the contiguous United States. J Hydrometeorol 20:1339–1357

Gimeno L, Drumond A, Nieto R, et al (2010) On the origin of continental precipitation. Geophys Res Lett 37:. https://doi.org/10.1029/2010gl043712

Gronewold AD, Bruxer J, Durnford D, et al (2016) Hydrological drivers of record-setting water level rise on Earth's largest lake system. Water Resour Res 52:4026–4042

Gronewold AD, Fortin V, Lofgren B, et al (2013) Coasts, water levels, and climate change: A Great Lakes perspective. Clim Change 120:697–711

Gronewold AD, Rood RB (2019) Recent water level changes across Earth's largest lake system and implications for future variability. J Great Lakes Res 45:1–3

Hayhoe K, VanDorn J, Croley T II, et al (2010) Regional climate change projections for Chicago and the US Great Lakes. J Great Lakes Res 36:7–21

Held IM, Soden BJ (2006) Robust responses of the hydrological cycle to global warming. J Clim 19:5686–5699

Jiang Z, Li W, Xu J, Li L (2015) Extreme precipitation indices over China in CMIP5 models. Part I: Model evaluation. J Clim 28:8603–8619

John A, Douville H, Ribes A, Yiou P (2022) Quantifying CMIP6 model uncertainties in extreme precipitation projections. Weather Clim Extrem 36:100435

Kayastha MB, Ye X, Huang C, Xue P (2022) Future rise of the Great Lakes water levels under climate change. J Hydrol (Amst) 612:128205

Kunkel KE, Yin X, Sun L, et al (2022) Extreme Precipitation Trends and Meteorological Causes Over the Laurentian Great Lakes. Hydroclimatology of the Great Lakes Region of North America

Lehner F, Deser C, Maher N, et al (2020) Partitioning climate projection uncertainty with multiple large ensembles and CMIP5/6. Earth Syst Dyn 11:491–508

Li C, Sinha E, Horton DE, et al (2014) Joint bias correction of temperature and precipitation in climate model simulations. J Geophys Res 119:13,153-13,162

Li L, Li W, Barros AP (2013) Atmospheric moisture budget and its regulation of the summer precipitation variability over the Southeastern United States. Clim Dyn 41:613–631

Li L, Li W, Kushnir Y (2012) Variation of the North Atlantic subtropical high western ridge and its implication to Southeastern US summer precipitation. Clim Dyn 39:1401–1412

Li M, Wu P, Ma Z, Liu J (2024) Climate change reshapes bioclimatic environments in China's dry–wet transition zones. J Hydrol (Amst) 634:131122

Li W, Li L, Fu R, et al (2011) Changes to the North Atlantic subtropical high and its role in the intensification of summer rainfall variability in the southeastern United States. J Clim 24:1499–1506

Mahony CR, Wang T, Hamann A, Cannon AJ (2022) A global climate model ensemble for downscaled monthly climate normals over North America. Int J Climatol 42:5871–5891

Malloy KM, Kirtman BP (2020) Predictability of Midsummer Great Plains Low-Level Jet and Associated Precipitation. Weather Forecast 35:215–235

McBean E, Motiee H (2008) Assessment of impact of climate change on water resources: a long term analysis of the Great Lakes of North America. Hydrology and Earth System Sciences 12:239–255

Minallah S, Steiner AL (2021a) Role of the atmospheric moisture budget in defining the precipitation seasonality of the Great Lakes region. J Clim 34:643–657

Minallah S, Steiner AL (2021b) Analysis of the Atmospheric Water Cycle for the Laurentian Great Lakes Region using CMIP6 models. J Clim 1–47

Nijsse FJMM, Cox PM, Williamson MS (2020) Emergent constraints on transient climate response (TCR) and equilibrium climate sensitivity (ECS) from historical warming in CMIP5 and CMIP6 models. Earth Syst Dyn 11:737–750

O’Gorman PA (2015) Precipitation extremes under climate change. Curr Clim Change Rep 1:49–59

O’Neill BC, Tebaldi C, van Vuuren DP, et al (2016) The Scenario Model Intercomparison Project (ScenarioMIP) for CMIP6. Geosci Model Dev 9:3461–3482

Paxton A, Schoof JT, Ford TW, Remo JWF (2021) Extreme precipitation in the great Lakes region: Trend estimation and relation with large-scale circulation and humidity. Front Water 3:. https://doi.org/10.3389/frwa.2021.782847

Peltier WR, d’Orgeville M, Erler AR, Xie F (2018) Uncertainty in future summer precipitation in the Laurentian Great Lakes basin: Dynamical downscaling and the influence of continental-scale processes on regional climate change. J Clim 31:2651–2673

Pendergrass AG, Lehner F, Sanderson BM, Xu Y (2015) Does extreme precipitation intensity depend on the emissions scenario? Geophys Res Lett 42:8767–8774

Pfahl S, O’Gorman PA, Fischer EM (2017) Understanding the regional pattern of projected future changes in extreme precipitation. Nat Clim Chang 7:423–427

PRISM Climate Group (2014) 30-year climate normals. 30-year climate normals, Oregon State University

Rey SJ, Anselin L (2010) PySAL: A Python Library of Spatial Analytical Methods. In: Fischer MM, Getis A (eds) Handbook of Applied Spatial Analysis: Software Tools, Methods and Applications. Springer Berlin Heidelberg, Berlin, Heidelberg, pp 175–193

Rodionov S (1994a) Association between winter precipitation and water level fluctuations in the Great Lakes and atmospheric circulation patterns. J Clim. https://doi.org/10.1175/1520-0442(1994)007<1693:ABWPAW>2.0.CO;2

Rodionov S, Assel R (2000) Atmospheric teleconnection patterns and severity of winters in the Laurentian Great Lakes basin. Atmosphere - Ocean 38:601–635

Rodionov S, Assel RA (2003) Winter severity in the Great Lakes region: a tale of two oscillations. Climate Research 24:19–31

Rodionov SN (1994b) Association between winter precipitation and water level fluctuations in the great lakes and atmospheric circulation patterns. J Clim 7:1693–1706

Seager R, Naik N, Vecchi GA (2010) Thermodynamic and dynamic mechanisms for large-scale changes in the hydrological cycle in response to global warming. J Clim 23:4651–4668

Seager R, Neelin D, Simpson I, et al (2014) Dynamical and thermodynamical causes of large-scale changes in the hydrological cycle over North America in response to global warming. J Clim 27:7921–7948

Shaw SB, Royem AA, Riha SJ (2011) The relationship between extreme hourly precipitation and surface temperature in different hydroclimatic regions of the United States. J Hydrometeorol 12:319–325

Shrestha NK, Seglenieks F, Temgoua AGT, Dehghan A (2022) The impacts of climate change on land hydroclimatology of the Laurentian Great Lakes basin. Front Water 4:. https://doi.org/10.3389/frwa.2022.801134

Srivastava A, Grotjahn R, Ullrich PA (2020) Evaluation of historical CMIP6 model simulations of extreme precipitation over contiguous US regions. Weather and Climate Extremes 29:100268

Steinschneider S, McCrary R, Mearns LO, Brown C (2015) The effects of climate model similarity on probabilistic climate projections and the implications for local, risk-based adaptation planning. Geophys Res Lett 42:5014–5044

Teale N, Robinson DA (2022) Long-term variability in atmospheric moisture transport and relationship with heavy precipitation in the eastern USA. Clim Change 175:. https://doi.org/10.1007/s10584-022-03455-3

Tokarska KB, Stolpe MB, Sippel S, et al (2020) Past warming trend constrains future warming in CMIP6 models. Sci Adv 6:. https://doi.org/10.1126/sciadv.aaz9549

Trenberth KE (2011) Changes in precipitation with climate change. Clim Res 47:123–138

Trenberth KE (1999) Conceptual framework for changes of extremes of the hydrological cycle with climate change. In: Weather and Climate Extremes. Springer Netherlands, Dordrecht, pp 327–339

Trenberth KE, Hoar TJ (1997) El Niño and climate change. Geophysical Research Letters. https://doi.org/10.1029/97GL03092

Tsonis AA, Hunt AG, Elsner JB (2003) On the relation between ENSO and global climate change. Meteorol Atmos Phys 84:229–242

United States EPA (2025) Great Lakes Facts and Figures. In: www.epa.gov. https://www.epa.gov/greatlakes/great-lakes-facts-and-figures. Accessed 5 Apr 2025

Vannière B, Demory M-E, Vidale PL, et al (2019) Multi-model evaluation of the sensitivity of the global energy budget and hydrological cycle to resolution. Clim Dyn 52:6817–6846

Wallace JM, Gutzler DS (1981) Teleconnections in the geopotential height field during the northern hemisphere winter. Mon Weather Rev 109:784–812

Wang C, Lee SK, Enfield DB (2007) Impact of the Atlantic warm pool on the summer climate of the Western Hemisphere. J Clim 20:5021–5040

Wang T, Hamann A, Spittlehouse D, Carroll C (2016) Locally downscaled and spatially customizable climate data for historical and future periods for north America. PLoS One 11:e0156720

Wei W, Li W, Deng Y, Yang S (2018) Intraseasonal variation of the summer rainfall over the Southeastern United States. Clim Dyn 0:0

Yang Z, Qian Y, Xue P, et al (2023) Moisture sources of precipitation in the Great Lakes Region: Climatology and recent changes. Geophys Res Lett 50:. https://doi.org/10.1029/2022gl100682

Yang Z, Wang J, Qian Y, et al (2024) Summer convective precipitation changes over the Great Lakes Region under a warming scenario. J Geophys Res 129:. https://doi.org/10.1029/2024jd041011

Zhang X, Alexander L, Hegerl GC, et al (2011) Indices for monitoring changes in extremes based on daily temperature and precipitation data. Wiley Interdiscip Rev Clim Change 2:851–870

Zhou W, Leung LR, Song F, Lu J (2021) Future changes in the great plains low-level jet governed by seasonally dependent pattern changes in the north Atlantic subtropical high. Geophys Res Lett 48:. https://doi.org/10.1029/2020gl090356

Zorzetto E, Li L (2021) Impacts of the North Atlantic Subtropical High on daily summer precipitation over the Conterminous United States. J Hydrometeorol. https://doi.org/10.1175/jhm-d-20-0242.1(Trenberth 2011)